THE EFFECT OF THE THERMOMECHANICAL PROCESSING ON THE MICROSTRUCTURE AND HARDNESS OF $(Co_{25}Cr_{15}Fe_{20}Ni_{40})_{83}Al_{17}$ HIGH ENTROPY ALLOY

Hüseyin Burak KOCABAŞ[1], Akın ÖZCAN[2], Hakan GAŞAN[3], Gül İpek SELİMOĞLU[4,*]
[1] *Eskisehir Technical University, Department of Material Science and Engineering, Eskisehir*
ORCID No: 0000-0002-1315-9171
[2] *Eskisehir Osmangazi University, Department of Metallurgical and Materials Engineering*
ORCID No: 0000-0002-7016-5519
[3] *Eskisehir Osmangazi University, Department of Metallurgical and Materials Engineering*
ORCID No: 0000-0003-0363-7173
[4] *Eskisehir Technical University, Department of Material Science and Engineering, Eskisehir*
ORCID No: 0000-0001-5752-7350

Keywords
Eutectic High Entropy Alloy
Vacuum Arc Melting
Rolling
Annealing

Abstract

$(Co_{25}Cr_{15}Fe_{20}Ni_{40})_{83}Al_{17}$ is a eutectic high entropy alloy (EHEA), which is composed of face centered cubic (FCC) and body centered cubic (BCC) phases. This dual (FCC+BCC) phase mixture provides good ductility and strength combination. In the scope of this study, it was aimed to analyze the effects of mechanical, thermal and thermomechanical processes on the microstructure and hardness of $(Co_{25}Cr_{15}Fe_{20}Ni_{40})_{83}Al_{17}$ EHEA, which was produced by the vacuum arc melting and casting method. With this aim, cold and hot rolling as well as different annealing treatments were applied to the as-cast plates. The cold-rolling was performed at room temperature while the hot rolling temperature was varied in between 500-1100 ℃. The maximum deformation that can be applied was 50% and 60 % after cold and hot rolling, respectively. Since the results of Rietveld analyses suggested that FCC content increases with increasing deformation temperature, the limited deformability was attributed to the deformation-induced ordering and/or local amorphization within FCC phase. The hardness was increased from 280 HV to 412 HV after 50% cold-rolling. A similar high hardness value (399 HV) was obtained after ~50% deformation at 750 ℃, indicating that the dynamic recrystallization had no significant effect up to 1100 ℃.

TERMOMEKANİK İŞLEMİN $(Co_{25}Cr_{15}Fe_{20}Ni_{40})_{83}Al_{17}$ YÜKSEK ENTROPİLİ ALAŞIMININ MİKROYAPISINA VE SERTLİĞİNE ETKİSİ

Anahtar Kelimeler
Ötektik Yüksek Entropili Alaşım
Vakum Ark Ergitme
Haddeleme
Tavlama

Öz

$(Co_{25}Cr_{15}Fe_{20}Ni_{40})_{83}Al_{17}$ yüzey merkezli kübik (FCC) ve hacim merkezli kübik (BCC) fazlardan oluşan bir ötektik yüksek entropili alaşımdır (EYEA). Bu ikili faz karışımı (FCC+BCC), iyi süneklik ve mukavemet kombinasyonu sağlar. Bu çalışma kapsamında, vakum ark ergitme ve döküm yöntemi ile üretilen $(Co_{25}Cr_{15}Fe_{20}Ni_{40})_{83}Al_{17}$ EYEA'nın mikroyapısı ve sertliği üzerine mekanik, termal ve termomekanik süreçlerin etkisinin incelenmesi amaçlanmıştır. Bu amaçla, döküm levhalara soğuk ve sıcak haddeleme ile farklı tavlama işlemleri uygulanmıştır. Soğuk haddeleme oda sıcaklığında yapılırken, sıcak haddeleme sıcaklığı 500-1100 ℃ arasında değiştirilmiştir. Soğuk ve sıcak haddeleme sonrasında uygulanabilen maksimum deformasyon sırasıyla %50 ve %60 olmuştur. Rietveld analizlerinin sonuçları, FCC miktarının artan deformasyon sıcaklığı ile arttığını gösterdiğinden, sınırlı deforme edilebilirlik, FCC fazında deformasyona bağlı düzenlenime ve/veya lokal amorfizasyona bağlanmıştır. %50 soğuk haddelemeden sonra sertlik 280 HV'den 412 HV'ye yükselmiştir. Benzer yüksek sertlik değeri (399 HV) 750 ℃'de ~%50 deformasyondan sonra elde edilmiştir ki bu da dinamik yeniden kristalleşmenin 1100 ℃'ye kadar belirgin bir etkisinin olmadığını göstermektedir.

Research Article
Submission Date : 13.06.2022
Accepted Date : 11.01.2023
* Corresponding author : gis@eskisehir.edu.tr

Araştırma Makalesi
Başvuru Tarihi : 13.06.2022
Kabul Tarihi : 11.01.2023
https://doi.org/10.31796/ogummf.1128421

1. Introduction

$(Co_{25}Cr_{15}Fe_{20}Ni_{40})_{83}Al_{17}$ is an eutectic high entropy alloy (EHEA), which is composed of face centered cubic (FCC) and body centered cubic (BCC) phases. This dual (FCC+BCC) phase mixture provides good ductility and strength combination (Yiping et al., 2014). In the scope of this study, the effects of cold and hot rolling as well as annealing on the microstructure and hardness of $(Co_{25}Cr_{15}Fe_{20}Ni_{40})_{83}Al_{17}$ alloy were investigated.

2. Literature Review

High entropy alloy (HEA) concept is a highly appealing topic for industry in recent years. This new design of alloying has successful outcomes in various fields considering their mechanical and physical properties, such as the unique wear resistance, excellent strength and thermal stability at elevated temperatures, superior elongation, great fatigue and fracture resistance (Tong et al., 2005; Senkov, Wilks, Scott and Miracle, 2011; Hemphill et al., 2012; Pickering and Jones, 2016).

The strength originated from BCC phase and the ductility originated from FCC phase were combined and optimized with eutectic high entropy concept (Yiping et al., 2014). Further improvements can be achieved by thermomechanical processing of EHEAs. Although there are limited studies in the literature, a brief review will be presented.

Bhattacharjee et al. (2018) studied the effects of cryo-rolling and annealing on the microstructure and mechanical properties of $AlCoCrFeNi_{2.1}$ EHEA. After multi-pass cryo-rolling, reduction in thickness up to 90% was achieved. The high-strength that was achieved after cryo-rolling resulted in brittleness of the alloy but after annealing at 800 °C for 1 hour, the alloy displayed a good combination of strength and ductility. In a similar study, Wani et al. (2017) studied the effect of cold-rolling and annealing on the microstructure and mechanical properties of $AlCoCrFeNi_{2.1}$ EHEA. They revealed that 90% cold-deformation has resulted in disordering of $L1_2$ phase while annealing resulted in the breakdown of lamellar eutectic microstructure. The warm-rolling of the same alloy was studied by Reddy et al. (2019) at different temperatures (400 °C, 600 °C and 750 °C). The deformation induced disordering of $L1_2$ phase was also detected after 90% deformation at 750 °C. Moreover, the fraction of FCC/$L1_2$ phase has decreased while nonlamellar structure became more dominant after deformation at 750 °C. High temperature deformation characteristics, on the other hand, was studied by Tian et al. (2020) for AlCoCrFeNi HEA. It was observed that the equiaxed dendritic microstructure after casting became elongated normal to the compressive direction while grain elongation extent increased with the increased strain rate. Moreover, σ and FCC phases in addition to A2+B2 structure of the as-cast alloy were detected after hot-deformation.

In a recent study, the effect of the interface coherency between FCC/BCC layers on the plastic deformation characteristics was investigated (Yang et al., 2023). It was shown that the coherency of the interphase has a crucial role in the plastic deformation mechanisms of EHEAs. If the interface between FCC and BCC phases is coherent, then co-deformation takes place by continuous slipping of dislocations while semi-coherent interface is an effective barrier to dislocation penetration from FCC to BCC and results in local deformation of FCC. Moreover, the deformation-induced amorphization was detected under high-plastic deformation in the case of semi-coherent interface, which results in a considerable strengthening effect.

Although there are researches on the deformation of EHEAs other than AlCoCrFeNi system (Li, Yiping, Wei, Zhiqiangi and Tingju, 2016; Jain, Rahul, Samal, Kumar and Phanikumar, 2020; Shah, Rahul, Bysahk, and Panikumar, 2021) detailed studies on the mechanisms are concentrated on AlCoCrFeNi systems (Li et al., 2021). In the scope of this study, a more complex alloy composition has been selected in order to contribute to the literature in terms of deformation characteristics of EHEAs, which is a recently developing research field.

3. Material and Methods

The phase diagram of $(Co_{25}Cr_{15}Fe_{20}Ni_{40})_{100-x}Al_x$, which was calculated by ThermoCalc (2017) TCHEA2 database, is given in Figure 1. The composition of the alloy was selected to be $(Co_{25}Cr_{15}Fe_{20}Ni_{40})_{83}Al_{17}$ in order to get a eutectic system since the studies on the deformation of eutectic HEAs (EHEAs) are still limited in literature. In this study, research and publication ethics were complied with.

Al, Co, Cr, Fe and Ni with at least 99.9 % purity (Alfa Aesar, USA) were vacuum arc melted and casted under argon atmosphere. In order to get homogenous structure, remelting were done for three times. The thickness of each casted plate was 6.6 mm while the width and length were 11.5 mm and 65 mm, respectively.

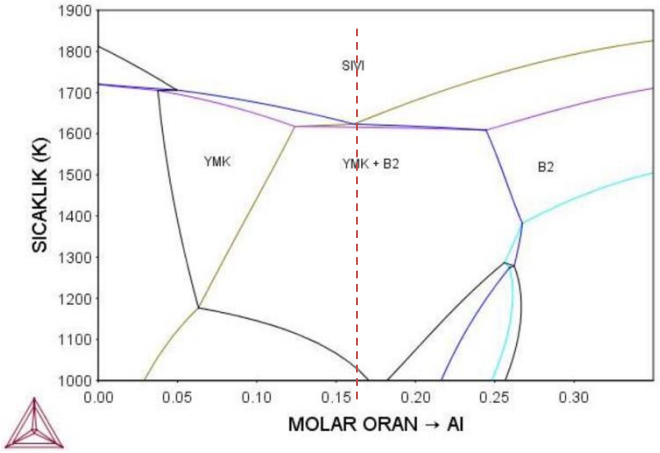

Figure 1. The Phase Diagram Of $(Co_{25}Cr_{15}Fe_{20}Ni_{40})_{100-x}$ Al_x

$(Co_{25}Cr_{15}Fe_{20}Ni_{40})_{83}Al_{17}$ EHEA plates were either rolled at room temperature and annealed afterwards or hot rolling was applied to observe the effect of dynamic recrystallization. The rolling has continued up to maximum deformation that can be attained at that temperature. Lab-scale roll-mill (Durston FSM160, England) was used for the deformation and the amount of deformation was calculated in terms of true strain using the reduction in the cross-sectional area of the plates. The annealing time after cold-rolling was kept constant at 1 hour. The maximum hot-rolling temperature, on the other hand, was selected to be 1100 °C since the melting temperature of the alloy is 1376 °C. All mechanical, thermal and thermomechanical processes were given in Table 1.

Table 1. All Processes That Were Applied on $(Co_{25}Cr_{15}Fe_{20}Ni_{40})_{83}Al_{17}$ EHEA Plates.

Treatment	Details
Cold Rolling	%50 Deformed
Annealing	%50 Deformed+ Annealed at 750 °C
	%50 Deformed+ Annealed at 1000 °C
Hot Rolling	%44 Deformed at 500 °C
	%53 Deformed at 750 °C
	%60 Deformed at 1100 °C

The metallographic specimen preparation was done with Struers automatic polishing machine and 25 vol. % nitric acidic solution (25 vol. % nitric acid + 75 vol. % distilled water) was used as etchant. All optical micrographs were taken at 200x magnification. Moreover, SEM (Zeiss, Supra 50VP, Oberkochen, Germany) with an energy-dispersive X-ray spectroscopy (EDX) attachment was employed for detailed microstructural characterization. SEM micrographs were taken with back-scattered electron (BSE) mode under 20 kV excitation voltage.

XRD analyses (MiniFlex600, Rigaku, Japan) were applied with Cu-Kα radiation at 40 kV and 15 mA and the scanning rate was 2°/min in between 30-90°. XRD analysis results of all plates were processed with Rietveld analysis to observe the change of the percentages of phases present.

The hardness measurements were done at the end of each process by using EMCO Test (Prüfmaschinen GmbH, Austria). Vickers micro-hardness measurements were taken under 10 kg force that is applied for 3 seconds and at least 5 measurements were taken to determine average micro-hardness values.

4. Results and Discussions

The microstructures of all alloys were generally consisted of lamellar eutectic structure as given in Figure 2. A line analysis (yellow line on Figure 2 (a)) was taken to determine the phases that constitutes the eutectic phase mixture. The phase having lighter color (seems to have higher level) was labelled as region A while the other one having darker color (seems to have lower level) was labelled as region B. The amounts of Al and Ni were observed to be increased in region B while the amounts of other elements were observed to be increased in region A as the result of EDX analysis (Figure 2(b)). Accordingly, lamellar structure was found to be consisted of FCC/L12 (region A) and BCC/B2 (region B) phases.

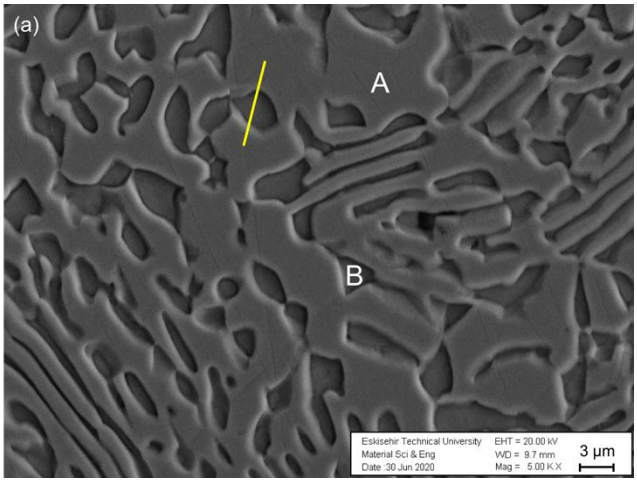

Figure 2. (a) SEM Micrograph (5000X) Showing Where EDX Line Analysis Was Taken.

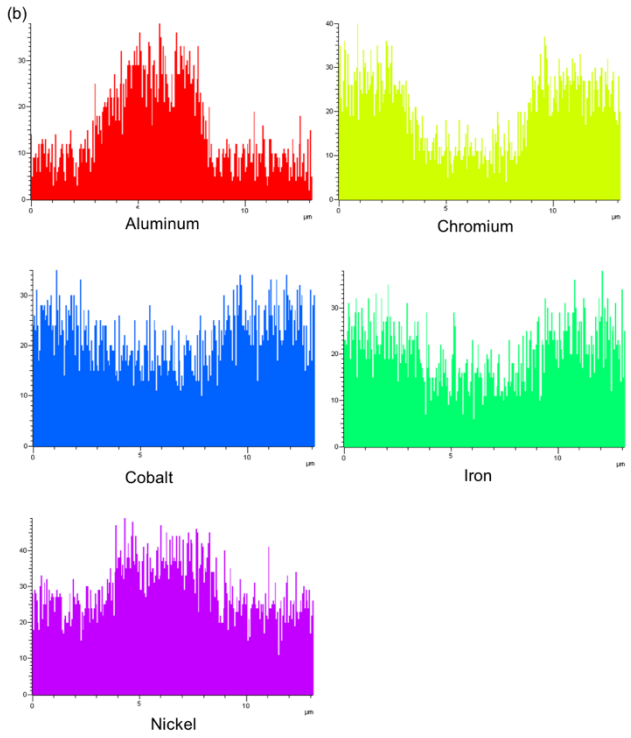

Figure 2. (b) The Results Of EDX Line Analysis, Where Red Belongs To Aluminum, Yellow Belongs To Chromium, Green Belongs To Iron, Blue Belongs To Cobalt And Pink Belongs To Nickel.

As it can be seen from Figure 3, the exact grain boundaries could not be distinguished, rather domain structures were detected in the microstructure of $(Co_{25}Cr_{15}Fe_{20}Ni_{40})_{83}Al_{17}$ alloys.

Figure 3. The Optical Micrograph Of As-Cast Alloy.

The microstructure of cold-rolled alloy was given in Figure 4. The refinement of the microstructure after cold-rolling is obvious in the optical micrograph. The black points in SEM micrograph, on the other hand, belong to casting porosities.

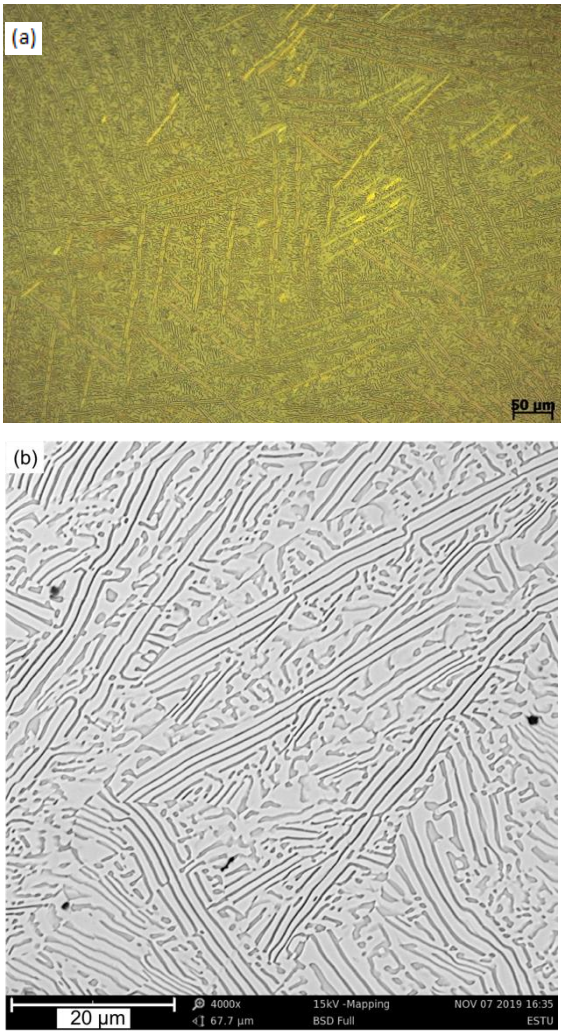

Figure 4. (a) Optical And (b) SEM Micrographs Of 50% Cold-Rolled Alloy (4000X).

The cold-rolled plates were annealed at 750 °C and 1000 °C, respectively (Figure 5). The lamellar structure was maintained after annealing. However, the edges of the lamellae were observed to change from planar to a more roughed structure.

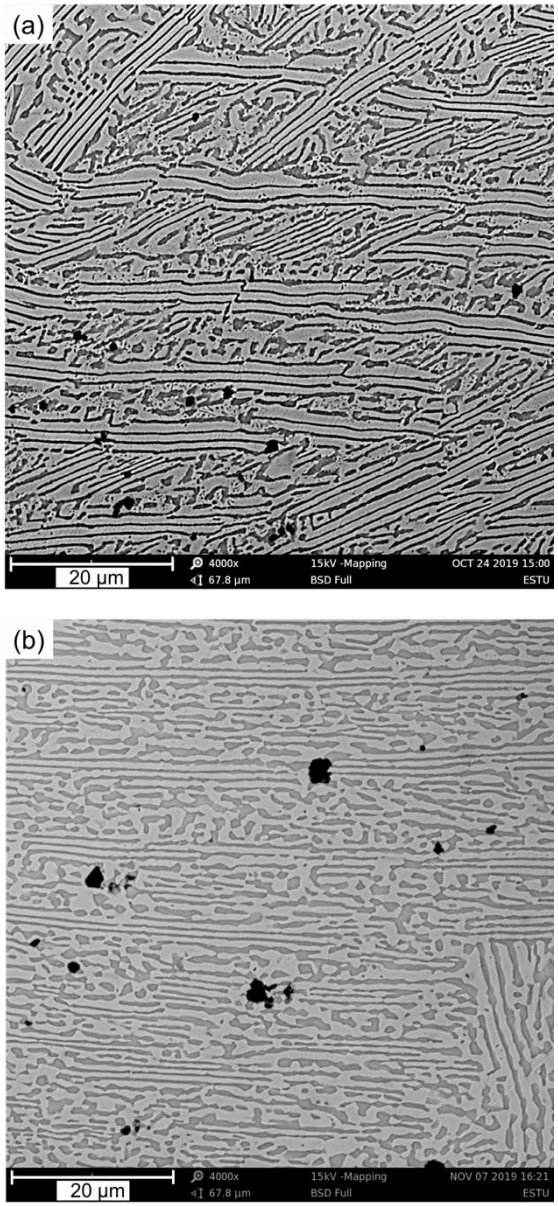

Figure 5. SEM Micrographs Of The Alloys, Which Were Annealed At (a) 750°C And (b) 1000°C, Respectively (4000X).

According to XRD analysis results, B2 peak was appeared at ~35° with the applied cold-rolling indicating a tendency towards ordering with deformation (Figure 6). Since ordered phases have lower deformability than disordered phases, this can be the reason of limited (maximum 50%) deformability during cold rolling. The peaks at ~45° and ~85°, on the other hand, have become more diffuse. This was attributed to increased dislocation density with the applied deformation.

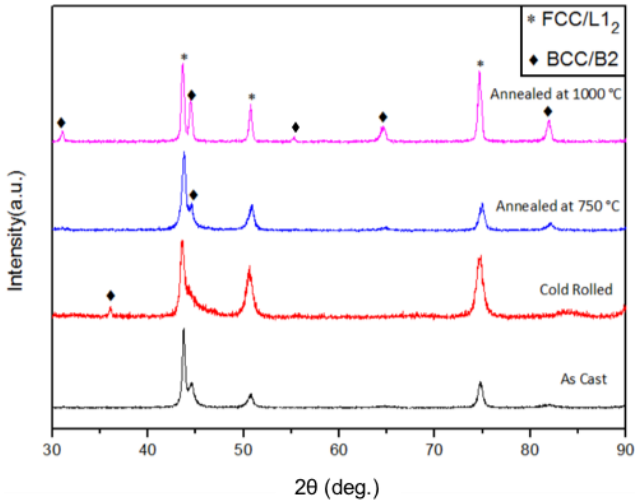

Figure 6. XRD Results Of As-Cast, Cold Rolled And Annealed Plates.

The Rietveld analyses (Table 2), on the other hand, indicated a slight decrease in FCC content after annealing.

Table 2. The Results Of Rietveld Analyses

Treatment	FCC / $L1_2$ (%)	BCC / B2 (%)
50% cold-rolled	70	30
Annealed at 750 °C	65	35
Annealed at 1000 °C	66	34
44% hot-rolled at 500 °C	68	32
53% hot-rolled at 750 °C	71	29
60% hot-rolled at 1100 °C	81	19

The microstructures after hot rolling at 500°C, 750°C, and 1100 °C were given in Figure 7. It was observed that the lamellar structure had become distorted with decreasing deformation temperature. Moreover, lamellae thicknesses were decreased with the increasing deformation temperature.

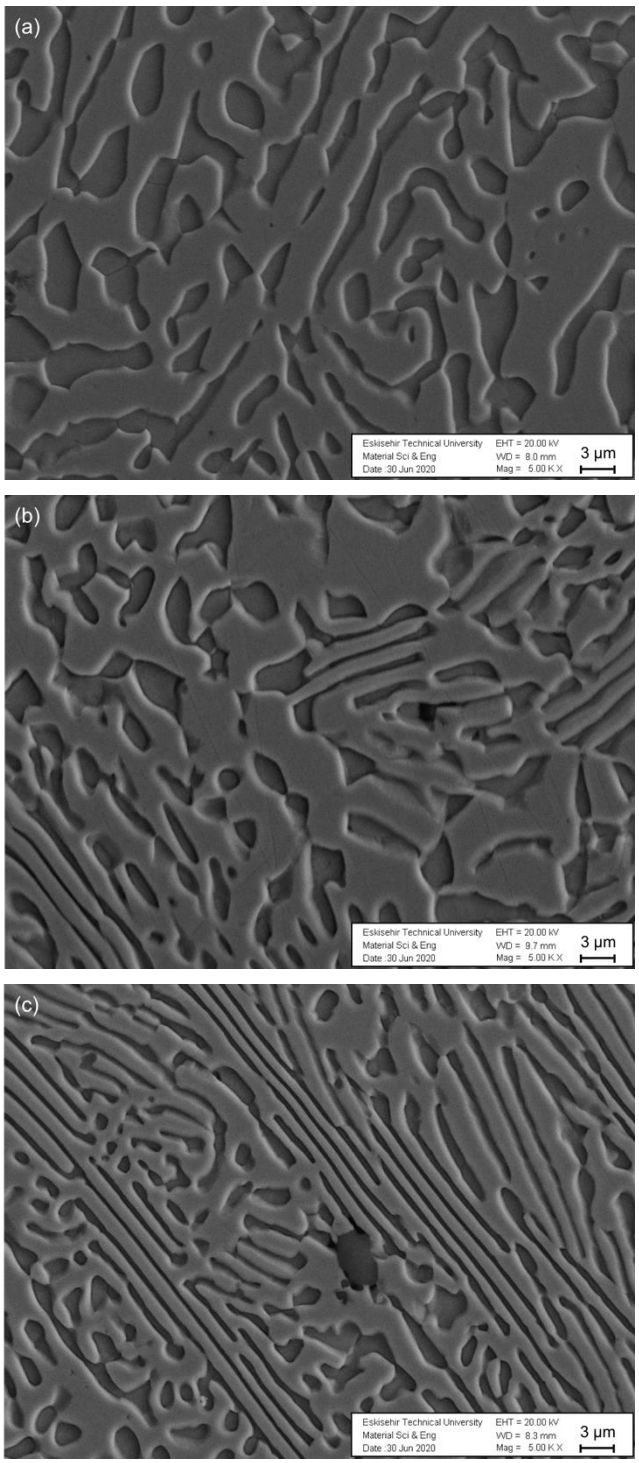

Figure 7. SEM Micrographs (5000X) Of The Alloys, Which Were Hot-Rolled At (a) 500 °C, (b) 750 °C And (c) 1100 °C, Respectively.

The results of XRD analyses after hot-rolling at various temperatures were given in Figure 8. The results obtained after hot-rolling at 500 °C were similar to that obtained after cold-rolling in terms of peak widening. This was attributed to the suppression of recrystallization due to the lower temperature of deformation. The fraction of BCC/B2 phase was observed to be decreasing with increasing deformation temperature according to the Rietveld analyses. The maximum deformability has increased with the increased temperature, as expected.

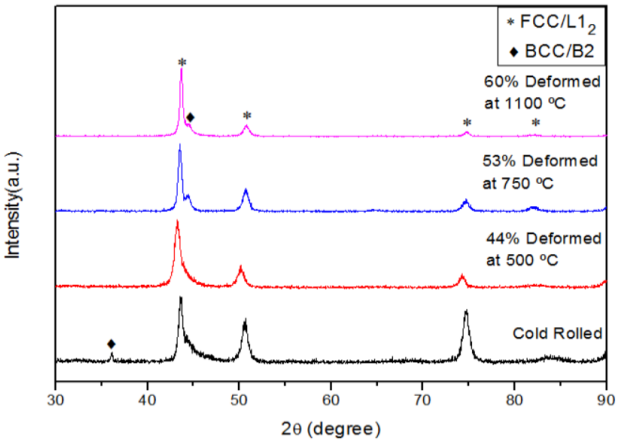

Figure 8. XRD Analyses Results Of Hot Rolled Plates (XRD Analysis Result of Cold Rolled Plate Was Added For Comparison).

The maximum deformation of 60% was attained after hot-rolling at 1100 °C. Although the FCC content of the alloy has increased with increasing deformation temperature (Table 2), the expected increase in deformability was not attained.

It was known that stacking fault energy (SFE) plays an important role in the deformation of FCC-based HEAs, especially when it is low (Su, Wu, Raabe and Li, 2019; Li, Zhao, Ritchie and Meyers, 2019; Paul, Tripathy, Saha and Bhattacharjee, 2023). Xu et al. (2021), on the other hand, revealed that SFE increases with increasing Al content while Deng et al. (2015) proposed increased Ni content also increases SFE. Since both Al and Ni contents of $(Co_{25}Cr_{15}Fe_{20}Ni_{40})_{83}Al_{17}$ is high, the effect of SFE was considered to be negligible on decreased deformability. Moreover, the deformation of dual-phase alloys commonly involves complex mechanisms and it was mentioned before that the nature of the interphase has a pronounced contribution (Yang et al., 2023). On the other hand, the formation of $L1_2$ nano-precipitates within FCC phase during low temperature annealing after cold-working has been reported (Gwalani et al., 2019). Accordingly, the deformation-induced ordering and/or amorphization can be the reasoning the behind the limited deformability.

Table 3. The Hardness of $(Co_{25}Cr_{15}Fe_{20}Ni_{40})_{83}Al_{17}$ EHEA Plates

Treatment	Hardness (HV)
As-cast	280 ±12
50% cold-rolled	412 ±7
Annealed at 750 °C	356 ±5
Annealed at 1000 °C	373 ±5
44% hot-rolled at 500 °C	393 ±8
53% hot-rolled at 750 °C	399 ±9
60% hot-rolled at 1100 °C	353 ±5

Table 3 shows the hardness values of the plates. The hardness was increased from 280 HV to 412 HV after cold-rolling as expected. The increase in hardness can both be attributed to increased dislocation density and stress-induced ordering. When the plates were annealed after cold-rolling, a decrease in hardness was observed but the hardness values were still higher with respect to that of as-cast plate. This can be due to the refinement of the structure as well as ordering of FCC phase, which cannot be detected with the available analysis methods.

The highest hardness among hot-rolled plates was measured after hot-rolling at 750°C. It was even higher when compared with the hardness of the plate, which was annealed at 750°C after cold-rolling, although having higher FCC content. This can be due to the balance between the generation of dislocations and the dynamic recrystallization. However, the ordering could also play a role in higher hardness. The presence of $L1_2$ phase can result in unusual variation of mechanical properties with temperature such as yield strength anomaly (Vikram et al., 2022). Transmission electron microscopy (TEM) analyzes to be performed at varying temperatures and/or under deformation can be enlightening about the origin of the results obtained.

5. Conclusions

In the scope of this study, the effects of cold and hot rolling as well as annealing on the microstructure and hardness of $(Co_{25}Cr_{15}Fe_{20}Ni_{40})_{83}Al_{17}$, which is a eutectic alloy, were investigated. It was chosen according to the relatively higher FCC content since FCC phase has higher ductility.

However, the maximum deformation of only 60% was attained after rolling at 1100 °C. Since the results of Rietveld analyses suggested that FCC content increases with increasing deformation temperature, the limited deformability was attributed to the deformation-induced ordering and/or local amorphization within FCC phase. Further studies, especially with TEM, have to be conducted in order to be certain about the origin of this phenomenon.

Although, the maximum deformation could not exceed 60%, the hardness values indicate the strengthening of $(Co_{25}Cr_{15}Fe_{20}Ni_{40})_{83}Al_{17}$ HEAs up to ~50% with thermomechanical treatment. Moreover, the information that has gained during this study, has given insight to the behavior of eutectic HEAs under mechanical and/or thermal processes.

Araştırmacıların Katkısı

Bu araştırmada; H.B. Kocabaş, bilimsel yayın araştırması, makalenin oluşturulması, haddeleme ve karakterizasyon çalışmalarında; A. Özcan, alaşımın üretimi ve Rietveld anlizlerinde ; H. Gaşan ve G.İ. Selimoğlu sonuçların yorumlanması ve makalenin oluşturulması konularında katkı sağlamışlardır.

Çıkar Çatışması

Yazarlar tarafından herhangi bir çıkar çatışması beyan edilmemiştir.

References

Bhattacharjee, T., Wani, I. S., Sheikh, S., Clark, I. T., Okawa, T., Guo, S., Bhattacharjee, S. & Tsuji, N. (2018). Simultaneous strength-ductility enhancement of a nano-lamellar $AlCoCrFeNi_{2.1}$ eutectic high entropy alloy by cryo-rolling and annealing. *Scientific Reports,* 8 (3276). doi : http://dx.doi.org/10.1038/s41598-018-21385-y

Deng, Y., Tasan, C.C., Pradeep, K.G., Springer, H., Kostka, A. & Raabe, D. (2015). Design of a twinning-induced plasticity high entropy alloy. *Acta Materialia*, 94, 124-133. doi: https://doi.org/10.1016/j.actamat.2015.04.014

Gwalani, B., Gangireddy, S., Zheng, Y., Soni, V., Mishra, R.S. & Banerjee, R. (2019) Influence of ordered $L1_2$ precipitation on strain-rate dependent mechanical behavior in a eutectic high entropy alloy. *Scientific Reports,* 9, 6371. doi: https://doi.org/10.1038/s41598-019-42870-y

Hemphill, M. A., Yuan, T., Wang, G. Y., Yeh, J. W., Tsai, C. W., Chuang, A. & Liaw, P. K. (2012). Fatigue behavior of $Al_{0.5}CoCrCuFeNi$ high entropy alloys. *Acta Materialia*, 60 (16), 5723–5734. doi: https://doi.org/10.1016/j.actamat.2012.06.046

Jain, R., Rahul, M.R., Samal, S., Kumar, V. & Phanikumar, G. (2020). Hot workability of Co–Fe–Mn–Ni–Ti eutectic high entropy alloy. *Journal of Alloys and Compounds*, 822, 153609. doi: https://doi.org/10.1016/j.jallcom.2019.153609

Li, J., Yiping, L., Wei, W., Zhiqiangi, C. & Tingju, L. (2016). Microstructure and Mechanical Properties of a $CoFeNi_2V_{0.5}Nb_{0.75}$ Eutectic High Entropy Alloy in As-cast and Heat-treated Conditions. *Journal of Materials Science and Technology,* 32 (3) 245 – 250. doi: https://doi.org/10.1016/j.jmst.2015.08.006

Li, W., Xie, D., Li, D., Zhang, Y., Gao, Y. & Liaw P.K. (2021). Mechanical behavior of high-entropy alloys. *Progress in Materials Science,* 118, 100777. doi: https://doi.org/10.1016/j.pmatsci.2021.100777

Li, Z., Zhao, S., Ritchie, R.O. & Meyers, M.A. (2019). Mechanical properties of high-entropy alloys with emphasis on face-centered cubic alloys. *Progress in Materials Science*, 102, 296-345. doi: https://doi.org/10.1016/j.pmatsci.2018.12.003

Paul, S., Tripathy, B., Saha, R. & Bhattacharjee, P.P. (2023). Microstructure and texture of heavily cold-rolled and annealed extremely low stacking fault energy Cr26Mn20Fe20Co20Ni14 high entropy alloy: Comparative insights. *Journal of Alloys and Compounds,* 930, 167418. doi: https://doi.org/10.1016/j.jallcom.2022.167418

Pickering, E.J. & Jones, N.G. (2016). High-entropy alloys: A critical assessment of their founding principles and future prospects. *International Materials Reviews*, 61(3), 183-202. doi: https://doi.org/10.1080/09506608.2016.1180020

Reddy, S.R., Yoshida, S., Sunkari, U., Lozinko, A., Joseph, J., Saha, R., Fabijanic, D., Guo, S., Bhattacharjee, P.P. & Tsuji, N. (2019). Engineering heterogeneous microstructure by severe warm-rolling for enhancing strength-ductility synergy in eutectic high entropy alloys. *Materials Science & Engineering A,* 764, 138226. doi: https://doi.org/10.1016/j.msea.2019.138226

Senkov, O.N., Wilks, G.B., Scott, J.M. & Miracle, D.B. (2011). Mechanical properties of $Nb_{25}Mo_{25}Ta_{25}W_{25}$ and $V_{20}Nb_{20}Mo_{20}Ta_{20}W_{20}$ refractory high entropy alloys. *Intermetallics*, 19 (5), 698-706. doi: https://doi.org/10.1016/j.intermet.2011.01.004

Shah, N., Rahul, M.R., Bysahk, S. & Panikumar, G. (2021). Microstructure stability during high temperature deformation of CoCrFeNiTa eutectic high entropy alloy through nano-scale precipitation. *Materials Science and Engineering: A,* 824, 141793. doi: https://doi.org/10.1016/j.msea.2021.141793

Su, J., Wu, X., Raabe, D. & Li, Z. (2019). Deformation-driven bidirectional transformation promotes bulk nanostructure formation in a metastable interstitial high entropy alloy. *Acta Materialia*, 167, 23-39. doi: https://doi.org/10.1016/j.actamat.2019.01.030

Tian, Q., Zhang, G., Yin, K. Wang, L., Wang, W., Cheng, W., Wang, Y. & Huang, J.C. (2020). High temperature deformation mechanism and microstructural evolution of relatively lightweight AlCoCrFeNi high entropy alloy. *Intermetallics*, 119, 106707. doi: https://doi.org/10.1016/j.intermet.2020.106707

Tong, C.J., Chen, M.R., Yeh, J.W. , Lin,S.J., Chen,S-K., Shun, T-T. & Chang,S-Y. (2005).Mechanical performance of the Al_xCoCrCuFeNi high-entropy alloy system with multiprincipal elements. *Metallurgical and Materials Transactions A*, 36A**,** 1263–1271. doi: https://doi.org/10.1007/s11661-005-0218-9

Vikram, R.J., Verma, S.K., Dash, K., Fabijanic, D., Murty, B.S. & Suwas, S. (2022). Mechanism Controlling Elevated Temperature Deformation in Additively Manufactured Eutectic High-Entropy Alloy. *Metallurgical And Materials Transactions A,* 53, 3681–3695. doi: https://doi.org/10.1007/s11661-022-06.777-0

Wani, I.S., Bhattacharjee,T., Sheikh,S., Lu,Y., Chatterjee, S., Guo, S. Bhattacharjee, P.P & Tsuji,N. (2017). Effect of severe cold-rolling and annealing on microstructure and mechanical properties of $AlCoCrFeNi_{2.1}$ eutectic high entropy alloy. *IOP Conf. Series: Materials Science and Engineering,* 194, 012018. doi: http://dx.doi.org/10.1088/1757-899X/194/1/012018

Xu, N., Yang, Z., Mu, X., Huang, Y., Li, S. & Wang, Y-D. (2021). Effect of Al addition on the microstructures and deformation behaviors of non-equiatomic FeMnCoCr metastable high entropy alloys. *Applied Physics Letters,* 119, 261902. doi: https://doi.org/10.1063/5.0069518

Yang, Z., Fu, B., Ning, Z., Bai, X., Yang, H., Chen, Q., Luo,D, Qui, N. & Wang, Y. (2023). Amorphization activated by semicoherent interfaces of FCC/BCC HEA multilayers during deformation. *Materials & Design,* 225, 111469. doi: https://doi.org/10.1016/j.matdes.2022.111469

Yiping, L., Yong, D., Sheng, G., Li, J., Huijun, K., Tongmin, W., Bin, W., Zhijun, W., Jinchuan, J., Zhiqiang, C., Haihui, R. & Tingju, L. (2014). A promising new class of high temperature alloys: Eutectic high-entropy alloys. *Scientific Reports,* 4 (6200). doi: http://dx.doi.org/10.1038/srep06200